Journal of Thrombosis and Haemostasis, **14**: 1803–1813 DOI: 10.1111/jth.13406

ORIGINAL ARTICLE

High-affinity von Willebrand factor binding does not affect the anatomical or hepatocellular distribution of factor VIII in rats

C. I. ØIE,* K. ROEPSTORFF,† C. BEHRENS,† J. BØGGILD KRISTENSEN,† D. M. KARPF,† G. BOLT,† C. N. GUDME,† M. KJALKE,† B. SMEDSRØD* and R. S. APPA†

**Vascular Biology Research Group, Department of Medical Biology, Faculty of Health Sciences, UiT The Arctic University of Norway, Tromsø, Norway; and †Novo Nordisk A/S, Novo Nordisk Park, Måløv, Denmark*

To cite this article: Øie CI, Roepstorff K, Behrens C, Bøggild Kristensen J, Karpf DM, Bolt G, Gudme CN, Kjalke M, Smedsrød B, Appa RS. High-affinity von Willebrand factor binding does not affect the anatomical or hepatocellular distribution of factor VIII in rats. *J Thromb Haemost* 2016; **14**: 1803–13.

Essentials

- Von Willebrand factor (VWF) stabilizes factor VIII (FVIII) and prevents its premature clearance.
- Rat anatomical and hepatocellular distribution studies assessed the VWF effect on FVIII clearance.
- Hepatocytes and liver sinusoidal endothelial cells play a key role in FVIII clearance.
- Anatomical and hepatocellular distribution of FVIII is independent of high-affinity VWF binding.

Abstract. *Background:* Von Willebrand factor (VWF) stabilizes factor VIII in the circulation and prevents its premature clearance. *Objective:* To study the effects of VWF on FVIII clearance in rats with endogenous VWF. *Methods:* Anatomical and hepatocellular distribution studies were performed in rats following intravenous administration of glycoiodinated recombinant FVIII (rFVIII) and a FVIII variant, FVIII-Y1680F, lacking high-affinity VWF binding. Radioactivity was quantified in organs, and in distinct liver cell populations. The role of VWF binding was also studied by immunohistochemical staining of rat livers perfused *ex vivo* with rFVIII alone or with a FVIII-binding VWF fragment. *Results:* The liver was the predominant organ of rFVIII distribution, and a radioactivity peak was also observed in the intestines, suggesting FVIII secretion to the bile by hepatocytes. In the liver, ~60% of recovered radioactivity was associated with hepatocytes, 32% with liver sinusoidal endothelial cells (LSECs), and 9% with Kupffer cells (KCs). When calculated per cell, 1.5-fold to 3-fold more radioactivity was associated with LSECs than with hepatocytes. The importance of hepatocytes and LSECs was confirmed by immunohistochemical staining; strong staining was seen in LSECs, and less intense, punctate staining in hepatocytes. Minor staining in KCs was observed. Comparable anatomical and hepatocellular distributions were observed with rFVIII and FVIII-Y1680F, and the presence of the VWF fragment, D'D3A1, did not change the FVIII staining pattern in intact livers. *Conclusions:* The present data support FVIII clearance via the liver, with hepatocytes and LSECs playing a key role. High-affinity VWF binding did not alter the anatomical or hepatocellular distribution of FVIII.

Keywords: distribution; hemophilia A; hepatocytes; immunohistochemistry; liver.

Correspondence: Rupa Shree Appa, Novo Nordisk A/S, Novo Nordisk Park, DK-2760 Måløv, Denmark.
Tel.: +45 30790916.
E-mail: rupa@novonordisk.com

Received 12 January 2016
Manuscript handled by: D. DiMichele
Final decision: P. H. Reitsma, 7 June 2016

Introduction

Factor VIII plays a critical role in the coagulation system [1], and a deficiency of FVIII results in impaired hemostasis, as seen in patients with hemophilia A [2]. The major site of FVIII biosynthesis is the liver, with liver sinusoidal endothelial cells (LSECs) having a primary role in producing and secreting FVIII [3–5]. FVIII associates with von Willebrand factor (VWF), which stabilizes FVIII and prevents its premature clearance [6,7], as demonstrated by the short half-life ($t_{1/2}$) of FVIII in the absence of VWF [8,9]. In humans, FVIII has a circulatory $t_{1/2}$ of ~12 h in the presence of VWF, whereas, in type 3 von Willebrand disease, the absence of VWF reduces the $t_{1/2}$ of infused FVIII to 2.5 h [7,10]. FVIII binds tightly to VWF, with a dissociation constant of 0.3 nM [11], leaving only 2–5% of FVIII not bound to VWF [12]. High-affinity binding of FVIII to VWF is dependent on sulfation of Tyr1680 [13,14], and

mutation of this residue results in faster clearance of FVIII and a subsequent reduction in plasma levels [13,15]. The majority of FVIII may be cleared in complex with VWF, as supported by the observation that decreased VWF clearance – seen as a reduction in the VWF propeptide to VWF antigen ratio – results in increased FVIII plasma levels [6].

Previous studies have demonstrated that both FVIII and VWF are primarily cleared via the liver [6,16], and identified Kupffer cells (KCs) and hepatocytes as the primary liver cell types responsible for FVIII uptake [16,17]. To further understand the clearance of FVIII in the presence and absence of VWF, anatomical and hepatocellular distribution studies were performed in rats, comparing ^{125}I-labeled recombinant FVIII (rFVIII) with FVIII-Y1680F, which has markedly reduced affinity for VWF [13,14]. Radioiodination of tyrosine residues, using the classic methods such as those involving lactoperoxidase [18], chloramine T [19] or iodogen, [20], results in randomly labeled proteins that are stable *in vivo* for no more than a few hours, as the ^{125}I can be rapidly cleaved off [21,22]. For the present study, a novel method of radioiodination, termed 'glycoiodination', was developed in order to follow FVIII for up to 16 h *in vivo*. In this method, a prosthetic ^{125}I-labeled group was selectively conjugated to the proteins' N-glycans, resulting in glycoiodinated rFVIII and FVIII-Y1680F molecules that were functionally active and resistant to deradioiodination over extended time frames *in vivo*. Although the loss of high-affinity binding to VWF decreased the $t_{1/2}$ of FVIII approximately four-fold in rats, it did not affect the anatomical or hepatocellular distribution of FVIII. Furthermore, the present studies indicate an important role for hepatocytes and LSECs in the clearance of FVIII, both in the presence and in the absence of high-affinity VWF binding.

Materials and methods

Proteins

The rFVIII used was turoctocog alfa (Novo Nordisk, Bagsværd, Denmark) [23]. The Y1680F substitution was introduced by modifying the turoctocog alfa-coding DNA by site-directed mutagenesis, and FVIII-Y1680F was produced as described previously [23]. The monomeric D′D3A1 VWF fragment comprising residues 764–1464 of full-length human VWF, and with Cys1099 and Cys1142 replaced by Ser, was produced in Chinese hamster ovary cells.

Radiolabeling

For *in vitro* studies, rFVIII and FVIII-Y1680F were labeled by use of the lactoperoxidase method (Fig. 1A) [18], and for *in vivo* studies, glycoiodination (Fig. 1B) was used. The glycoiodination method is based on site-selective conjugation of *in vivo*-stable prosthetic iodo−aromatic groups similar to those developed by Wilbur *et al*. [24] and Vaidyanathan *et al*. [25]. rFVIII and FVIII-Y1680F were desialylated by neuraminidase treatment, and resialylated with an aminooxy-modified cytidine-5′-monophospho-*N*-acetylneuraminic acid derivative, by use of the N-glycan-specific sialyltransferase ST3GalIII. ^{125}I was introduced in the *para* position of the aromatic prosthetic moiety 4-bromo-*N*-(4′,4′-dimethoxybutyl)benzamide, and this was followed by acetal deprotection and HPLC purification, resulting in pure 4-^{125}I-iodo-*N*-(4′-oxobutyl)benzamide. Specific oxime ligation of 4-^{125}I-iodo-N-(4′-oxobutyl)benzamide to the N-glycan aminooxy-derivatized rFVIII and FVIII-Y1680F resulted in the final products. Labeled proteins were diluted to 23 μCi mL^{-1} in 20 mM imidazole, 10% glycerol, 150 mM NaCl, 10 mM $CaCl_2$, 0.02% Tween-80, and 0.1% human albumin (pH 7.3).

Activity and ELISAs

rFVIII and FVIII-Y1680F antigen and activity before and after labeling were measured with Asserachrom ELISA (American Diagnostica, Lexington, MA, USA) and FVIII Coatest SP (Chromogenix, Diapharma, West Chester, OH, USA), respectively. The ability of rFVIII and FVIII-Y1680F to bind VWF was tested with ELISA [26]. Data were background-subtracted and fitted with an equation for log(agonist) versus response (four-parameter fit) with GRAPHPAD PRISM v.6.05.

In vitro *cell-binding assays*

The influence of VWF on rFVIII and FVIII-Y1680F *in vitro* cell binding was evaluated with a human glioblastoma cell line, U87 MG (ATCC; HTB-14), expressing high amounts of LDL receptor-related protein (LRP). Cells were maintained in advanced minimum essential medium (Gibco, Jupiter, FL, USA) supplemented with 10% fetal bovine serum and 1% penicillin–streptomycin. Cells were seeded in fibronectin-coated wells to 95% confluency. Cells were washed with HEPES-buffered saline (HBS) (100 mM HEPES, 150 mM NaCl, 4 mM KCl, 11 mM glucose, 5 mM $CaCl_2$, 1 mg mL^{-1} bovine serum albumin [BSA], pH 7.4), and incubated for 1 h at 37 °C with 1 nM ^{125}I–labeled rFVIII or FVIII-Y1680F – alone, with VWF (2.5–50 nM), or with 10 μg mL^{-1} of an anti-FVIII-C1 antibody (hF8-4F30; Novo Nordisk). Unbound material was removed with ice-cold HBS, and surface−bound radioactivity was released by incubation for 30 min, on ice, with 50 μg mL^{-1} trypsin, 50 μg mL^{-1} proteinase K and 5 mM EDTA in phosphate-buffered saline. After 5 min centrifugation at 290 × *g*, radioactivity in the supernatant was quantified in a gamma counter (Perkin Elmer, Waltham, MA, USA).

Experimental animals

Sprague-Dawley male rats (mean body weight, 250 g; Taconic, Ejby, Denmark) were housed under controlled conditions (20–23 °C; relative humidity, 30–65%; 12-h

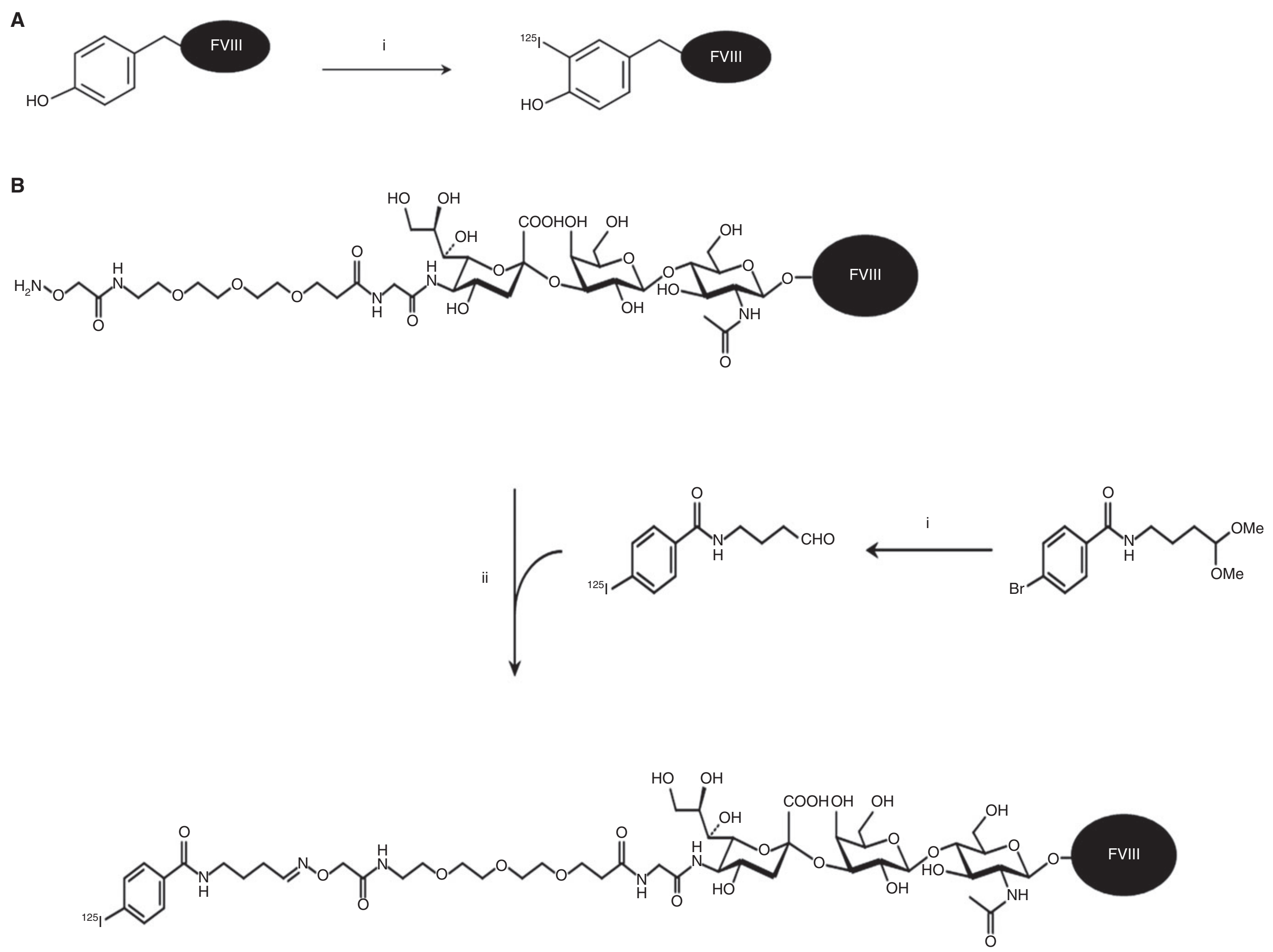

Fig. 1. Lactoperoxidase and glycoiodination methods for FVIII labeling. (A) Radiolabeling of FVIII tyrosines. (i) FVIII in imidazole buffer, $Na^{125}I$. Lactoperoxidase and hydrogen peroxide were incubated at room temperature for 30 min. (B) Glycoiodination method. 4-^{125}I-iodo-*N*-(4-oxobutyl)benzamide was produced from 4−bromo−*N*−(4′,4′−dimethoxybutyl)benzamide and $Na^{125}I$ by Br–I halogen exchange (i). The ^{125}I−labeled precursor was then incubated overnight at room temperature with aminooxy−modified recombinant FVIII (ii).

light/12-h dark cycle), and fed standard chow *ad libitum*. Pharmacokinetic (PK) and immunohistochemical studies were performed and approved by the Danish Government Animal Experiments Inspectorate and the Novo Nordisk Ethical Review Committee. Rats were anesthetized with 4% isoflurane (Abbott Scandinavia AB, Solna, Sweden) at time-points for liver harvesting, and maintained at 2.1%, or injected intravenously with a mixture of fentanyl/fluanisone (Hypnorm; VetaPharma, Elmet, Leeds, UK) and midazolam (Dormicum; Roche, Basel, Switzerland). For the anatomical and hepatocellular distribution studies, protocols were approved and conducted in accordance with the Norwegian National Animal Research Authority and Novo Nordisk Ethics Committee.

Pharmacokinetics

Rats received a single intravenous tail vein injection of ^{125}I-labeled rFVIII (200 IU kg^{-1}, n = 2) or unlabeled rFVIII (132 IU kg^{-1}, n = 3), and labeled or unlabeled FVIII-Y1680F (216 IU kg^{-1}, n = 4). Blood was sampled from the tail vein before dosing and up to 12 h after dosing for rFVIII, and up to 4 h for FVIII-Y1680F. Blood was stabilized in sodium citrate (0.013 M), diluted in FVIII Coatest SP buffer (50 mM Tris-HCl, 1% BSA, 10 mg L^{-1} ciprofloxacin, pH 7.3), and centrifuged 5 min at 4000 × g. FVIII antigen in supernatants was analyzed with ELISA, as described previously [27]. The percentage of protein-associated radioactivity was calculated from the total radioactivity and the amounts in supernatants and precipitates following trichloroacetic acid precipitation [28–30].

Anatomical distribution

The anatomical distribution of rFVIII and FVIII-Y1680F was investigated as described previously [31]. ^{125}I-labeled rFVIII or FVIII-Y1680F (135 IU kg^{-1}) was diluted in physiologic saline, and administered intravenously to rats via the lateral tail vein. At 1 h, 8 h and 16 h after injection (rFVIII) and at 0.5 h and 1 h after injection (FVIII-

Y1680F), rats were subcutaneously injected with a mixture of 0.4 mg kg^{-1} Dormitor (Orion Pharma, Newbury, Berkshire, UK) and 60 mg kg^{-1} Ketalar (Pfizer AS, Sandwich, Kent, UK). Blood (25 μL) was sampled from the tail tip. Before organ harvesting, blood was flushed out by perfusion of the heart with 0.9% saline, and the amount of radioactivity was measured in the liver, spleen, kidneys, stomach, intestines, urine, bladder, lungs, heart, brain, tail, muscle, thyroid, testicles, and adrenals. Total blood radioactivity was calculated from the blood sample, based on the estimation that rats contain ~ 7 mL of blood per 100 g of body weight [32].

Hepatocellular distribution determined by cell isolation

Rats were dosed as described above. At 1 h and 7 h (rFVIII) or 0.5 h, 1 h and 2 h (FVIII-Y1680F) after injection, livers were perfused with collagenase to extract liver cells, and this was followed by sequential centrifugations, 2 min at 50 × *g* to obtain hepatocytes, and Percoll gradient, 30 min at 750 × *g* to obtain LSECs and KCs, as described previously [33–36]. LSEC preparations were between 95% and 98% pure, and the degree of LSEC contamination in KCs was < 10%, as assessed by light microscopy [37]. Hepatocytes and LSECs in suspension, and adherent KCs solubilized in 1% SDS, were analyzed for radioactivity, and the amount of radioactivity per million cells was calculated. The uptake per total cell population was assessed according to the relative numbers of hepatocytes, LSECs and KCs (7.6 : 2.5 : 1) in intact rat livers [38].

Hepatocellular distribution determined by immunohistochemistry (IHC)

By use of a previously described perfused rat liver model [39], rFVIII (20 nM) was added to the perfusate buffer and recirculated through the liver for 60 min. The liver was perfusion fixated by perfusion with 4% paraformaldehyde, and slices from the top lobe were processed for histology and embedded in paraffin. Sections (3 μm) were stained with a mouse anti-human FVIII mAb (FVIII-3F15; Novo Nordisk), and visualized by peroxidase-conjugated avidin–biotin complex (Vectastain; Vector Laboratories, Orton Southgate, Peterborough, UK) and an indirect biotin-conjugated tyramide signal amplification (TSA) system (Perkin Elmer) and diaminobenzidine (Sigma-Aldrich, St Louis, MO, USA). For double immunofluorescence staining, rFVIII was visualized with streptavidin–AlexaFluor 594 (Invitrogen, Carlsbad, CA, USA). rFVIII-stained sections were further stained for CD31 (rabbit polyclonal antibody; LifeSpan Biosciences, Seattle, WA, USA) or CD68 (mouse mAb; Abcam, Cambridge, Cambridgeshire, UK). CD31 was detected with a biotinylated donkey anti-rabbit secondary antibody (Jackson ImmunoResearch, Newmarket, Suffolk, UK), and TSA-AlexaFluor 488, and CD68 was detected with goat anti-rabbit AlexaFluor 488 (Invitrogen). A second round of heat-induced epitope retrieval was applied between rFVIII staining and CD31/CD68 staining to avoid cross-reactivity. No staining was observed when the primary antibodies were replaced with unspecific IgG (data not shown).

Statistical analysis

An unpaired, two-sided Student's *t*-test was performed to compare time-points and treatments for anatomical and hepatocellular distribution. *P*-values of < 0.05 were considered to be statistically significant.

Results

In vitro *characterization of rFVIII and FVIII-Y1680F*

The radiochemical purity of glycoiodinated proteins was >94%, and the specific radioactivity was 1–6 μCi μg^{-1}. Specific FVIII activity was 60–77% after glycoiodination, as compared with the unlabeled molecules. The binding of rFVIII and FVIII-Y1680F to VWF was evaluated with ELISA (Fig. 2A). The half-maximal binding of rFVIII was 0.19 ± 0.05 nM, whereas that of FVIII-Y1680F was 75 ± 28 nM (mean ± standard deviation; $n = 3$), confirming reduced affinity of FVIII-Y1680F for VWF. Consequently, FVIII-Y1680F cell binding was minimally affected by the presence of VWF, in contrast to that of rFVIII (Fig. 2B). At a physiologically relevant concentration of VWF (50 nM), the cell binding of rFVIII was reduced by 68% ± 4%, whereas that of FVIII-Y1680F was reduced by only 25% ± 14%. VWF inhibited ^{125}I-rFVIII internalization to the same extent as binding (data not shown). Preincubation with a C1 antibody that is known to prevent cell binding of FVIII [40] inhibited FVIII-Y1680F cell binding to a level similar to that observed for VWF inhibition of rFVIII, indicating that the specific binding of both proteins was comparable. Together, these data confirm that VWF binding of FVIII-Y1680F was impaired, resulting in a markedly reduced influence of VWF on FVIII-Y1680F cellular uptake.

Residual FVIII binding to immobilized human VWF was quantified following incubation of rFVIII (2 nM; corresponding to the maximal plasma concentration following the doses used in the rat studies) with plasma containing rat or human VWF (Fig. S1). Rat and human plasma inhibited rFVIII binding to immobilized VWF equally well, demonstrating binding of human rFVIII to rat VWF. Rat plasma samples with and without FVIII were also compared (Fig. S1B). Similar dose responses were observed for the two plasma samples, demonstrating that the capacity of rFVIII to bind to endogenous rat VWF is not influenced by endogenous rat FVIII.

Pharmacokinetics of radiolabeled rFVIII and FVIII-Y1680F

Radioiodination stability was compared between unlabeled rFVIII, glycoiodinated rFVIII and lactoperoxidase-

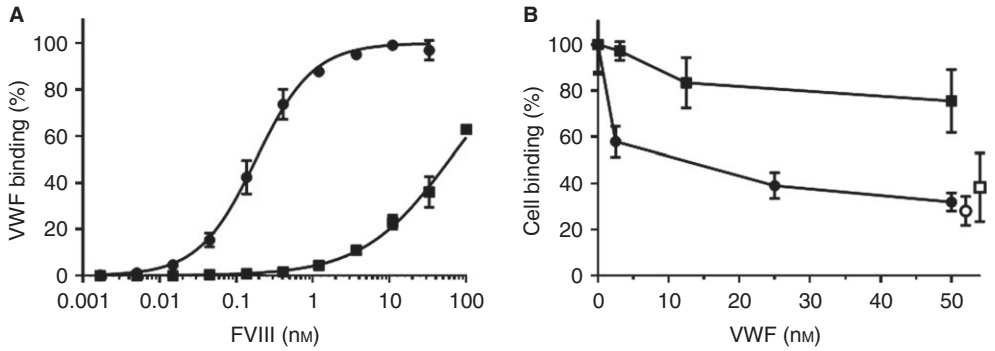

Fig. 2. von Willebrand factor (VWF) had a minimal effect on cell binding of FVIII-Y1680F. (A) The binding of recombinant FVIII (rFVIII) (circles) and FVIII-Y1680F (squares) to immobilized VWF was measured with ELISA. Data are mean ± standard deviation (SD); $n = 3$ individual experiments, each with duplicate determinations. (B) Cell binding of ^{125}I-rFVIII (circles) and ^{125}I-FVIII-Y1680F (squares) was investigated in the presence and absence of VWF. ^{125}I-rFVIII and ^{125}I-FVIII-Y1680F were incubated for 1 h at 37 °C with U-87 MG cells and varying concentrations of VWF. Cell binding in the presence of a C1 antibody (known to block cell binding) is indicated by open circles for rFVIII and open squares for FVIII-Y1680F. Data are mean ± SD for FVIII-Y1680F ($n = 3$) and rFVIII ($n = 6$), each with triplicate determinations. Data are depicted as percentage of cell uptake for the individual proteins.

Table 1 Estimated pharmacokinetic (PK) parameters of glycoiodinated and unlabeled recombinant factor VIII (rFVIII) and FVIII-Y1680F

	$t_{1/2}$ (h)	MRT (h)	CL (mL h^{-1} kg^{-1})
rFVIII ($n = 3$)	4.5 (3.1–6.5)	6.3 (4.3–9.0)	2.1 (1.8–2.3)
^{125}I-rFVIII ($n = 2$)	5.7 (4.5–6.7)	7.8 (6.1–9.5)	2.6 (2.1–3.1)
FVIII-Y1680F ($n = 4$)	1.2 (1.1–1.4)	1.7 (1.6–1.9)	68 (51–80)
^{125}I-FVIII-Y1680F ($n = 4$)	1.3 (1.25–1.34)	1.8 (1.7–1.9)	68 (61–82)

CL, clearance; MRT, mean residence time; $t_{1/2}$, half-life. Unlabeled rFVIII and FVIII-Y1680F and their ^{125}I-labeled counterparts, ^{125}I-rFVIII and ^{125}I-FVIII-Y1680F, were administered intravenously to rats, and FVIII activity was measured in plasma samples. Mean (range) PK parameters were estimated by non-compartmental analysis.

labeled rFVIII in rats. PK parameters showed that glycoiodination did not alter the FVIII antigen plasma concentration profile of rFVIII (Fig. S2), but, as predicted, a greater amount of radioiodinated protein than of lactoperoxidase-labeled rFVIII was circulating 12 h after dosing (93% versus 77%; Fig. S3). PK (rat) parameters of glycoiodinated rFVIII and FVIII-Y1680F were also comparable to those of their unlabeled counterparts (Table 1). Together, these data support the reliability of glycoiodination for use in distribution studies.

Anatomical distribution

The effect of VWF on FVIII distribution was investigated in an anatomical distribution study in rats, in which the influence of high-affinity VWF binding was explored with rFVIII and FVIII-Y1680F. Rats were dosed intravenously with 135 IU kg^{-1} rFVIII or FVIII-Y1680F. At 1 h, 8 h and 16 h (rFVIII) or 0.5 h, 1 h and 2 h (FVIII-Y1680F), blood was sampled and flushed from the body, and organs harvested. More than 94% of the radioactivity remained protein-bound for both rFVIII and FVIII-Y1680F, and <1% radioactivity was found in the thyroid at all time-points, demonstrating that the labeled FVIII molecules were minimally susceptible to deradioiodination *in vivo*.

At 1 h, 8 h and 16 h after injection with rFVIII, 51% ± 1%, 29% ± 4% and 10% ± 0.3% radioactivity was recovered, respectively. Figure 3 shows the anatomical distribution data presented as percentage of recovered radioactivity. Radioactivity found in the blood declined over time, from 61% at 1 h to 17% at 16 h after injection. Among the organs assessed, FVIII was primarily found in the liver; 30% of the recovered radioactivity was found in the liver at 1 h, declining to 15% and 6% at 8 h and 16 h, respectively (Fig. 3A). The organs with the second highest amount of recovered radioactivity were the intestines (small and large), where 3.2% was detected after 1 h; the recovered radioactivity increased to 30% at 8 h, declining thereafter to 11% by 16 h. When the radioactivity per gram of tissue was calculated, high concentrations of rFVIII were also detected in the spleen. The ratio of radioactivity recovered per gram of tissue, spleen to liver, was between 0.6 (at 1 h) and 1.7 (at 8 h and 16 h).

Owing to the faster clearance of FVIII-Y1680F, its anatomical distribution was assessed only up to 1 h after injection. A total of 52% of the dosed radioactivity was recovered 1 h after injection. Between 0.5 h and 1 h, radioactivity in the blood declined from 68% to 53%, and a comparable distribution among other organs was

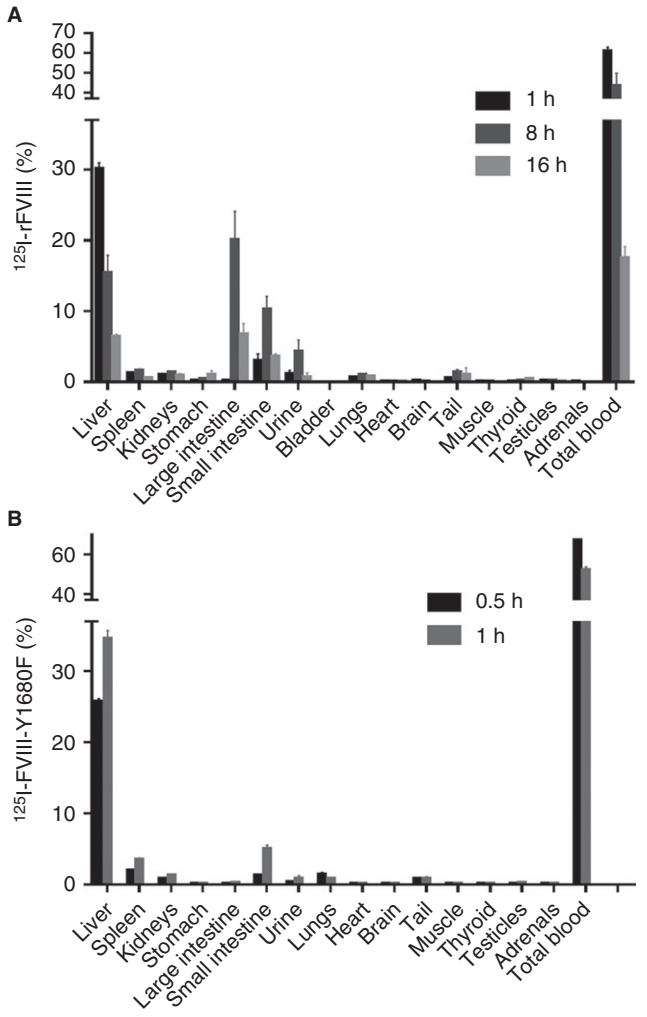

Fig. 3. The liver was the primary organ of distribution for recombinant FVIII (rFVIII) and FVIII-Y1680F. An anatomical distribution study of rFVIII and FVIII-Y1680F was performed in rats dosed intravenously with 135 U kg^{-1} ^{125}I-rFVIII (A) or ^{125}I–FVIII-Y1680F (B). Perfusion with physiologic saline via the heart flushed blood from the circulation, and organs were harvested at 1 h, 8 h and 16 h for rFVIII (A) and 0.5 h and 1 h for FVIII-Y1680F (B). Data (n = 3 per group) are presented as mean ± standard deviation of the percentage of radioactivity counted in the organ, in relation to the total radioactivity recovered.

observed for FVIII-Y1680 and rFVIII, with the liver being the primary organ of distribution (Fig. 3B). At 0.5 h after injection, 25% of the recovered radioactivity was in the liver, increasing to 34% at 1 h. Some radioactivity was also found in the intestines (1.5% at 0.5 h, and 5% at 1 h) and in the spleen. The ratio of radioactivity per gram of tissue, spleen to liver, was ~1.6 at all time-points.

The anatomical distribution of FVIII-Y1680F (280 IU kg^{-1}) was assessed at 1 h and 2 h time-points in separate experiments (two different doses: 135 IU kg^{-1} and 240 IU kg^{-1}) to confirm that the distribution patterns were similar beyond one half-life. The data were comparable to the data obtained at earlier time-points (Fig. 3B), as the liver contained the most radioactivity at 1 h and 2 h (42% and 46%, respectively), with additional radioactivity in the intestines (5–12%), kidney (2%), and spleen (4%), and <1% in all other organs at both time-points. The ratio of radioactivity per gram of tissue, spleen to liver, was the same as for rFVIII, being ~1.6 at both time-points.

Hepatocellular distribution

To investigate the types of liver cell that are responsible for the clearance and metabolism of FVIII, two different hepatocellular distribution studies were performed. First, FVIII was quantified in different cell types isolated from the liver after intravenous administration of ^{125}I-rFVIII or ^{125}I-FVIII-Y1680F. Second, FVIII was visualized by IHC in intact livers perfused *ex vivo* with rFVIII.

For the first study, hepatocytes, KCs and LSECs were isolated at different time-points from rat livers, and the radioactivity associated with each cell type was determined [38]. The hepatocellular distribution of radioactivity from rFVIII 1 h after administration was 60% ± 19% associated with hepatocytes, 32% ± 13% associated with LSECs, and 9% ± 7% associated with KCs (Fig. 4A). Seven hours after administration, the relative distribution of radioactivity from rFVIII between cell types was unchanged. A comparable hepatocellular distribution to that for rFVIII was observed with FVIII-Y1680F (Fig. 4B). At 1 h, most of the radioactivity was associated with hepatocytes (57% ± 9%), followed by LSECs (40% ± 8%), with the lowest levels in KCs (3% ± 3%). These percentages were also representative of data obtained at other time-points. When data were calculated as the amount of radioactivity per million cells, 2.5 times more radioactivity from rFVIII was associated with LSECs than with hepatocytes ($P < 0.01$) at 7 h. Similar results were obtained for FVIII-Y1680F; 1.5–3.0 times more radioactivity was associated with LSECs than with hepatocytes ($P < 0.05$) at all time-points after injection, indicating that, in addition to hepatocytes, LSECs have a predominant role in FVIII clearance, independently of high-affinity VWF binding.

Next, the hepatocellular distribution was examined in intact livers by IHC. As FVIII could not be detected by IHC at the doses previously used (135 IU kg^{-1}, corresponding to ~10 μg kg^{-1}), an *ex vivo* rat liver perfusion model was used (Fig. S4). This model allows higher doses of FVIII to be administered than in *in vivo* models, and delivers FVIII to the liver only. Histologic sections of the perfused livers were stained with an anti-human rFVIII antibody that does not stain endogenous rat FVIII, as confirmed in livers perfused only with buffer (Fig. 5D). The influence of VWF on FVIII uptake was addressed by comparing rat livers perfused with rFVIII (20 nM), with or without a five-fold molar excess of a VWF fragment, D′D3A1, containing the FVIII-binding domains of VWF (D′D3) [41]. This D′D3A1 fragment decreased FVIII

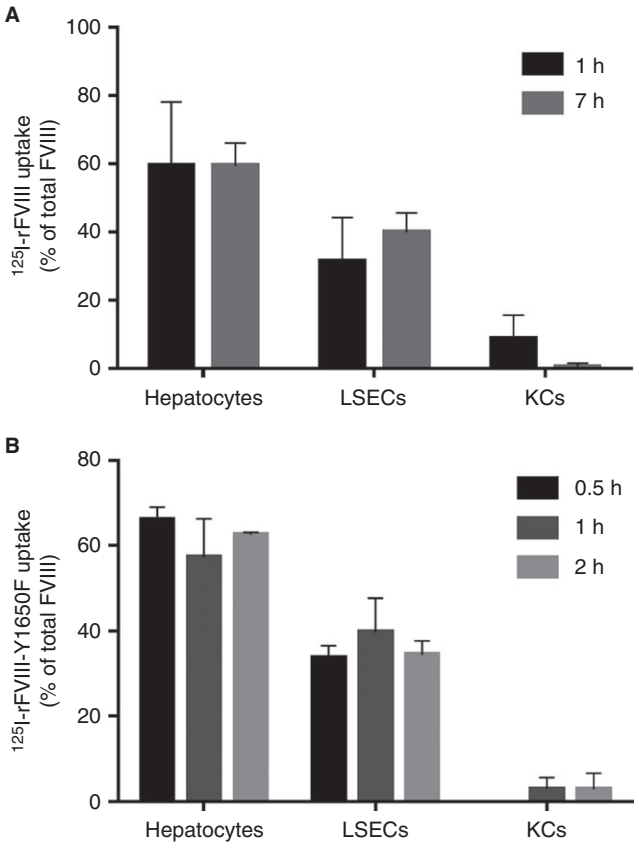

Fig. 4. Recombinant FVIII (rFVIII) and FVIII-Y1680F were primarily associated with hepatocytes and liver sinusoidal endothelial cells (LSECs). ^{125}I-rFVIII (A) and ^{125}I-FVIII-Y1680F (B), both dosed at 135 IU kg^{-1}, were administered intravenously to rats (n = 3 per time-point, with the exception of the 2-h time-point, where n = 2 for FVIII-Y1680F). At the time-points indicated, rats were anesthetized, and liver cells were isolated by collagenase perfusion of the liver and Percoll density gradient separation. Accumulation of radioactivity in each liver cell population was calculated on the assumption that liver uptake of FVIII was according to the cell ratio of 7.6 : 2.5 : 1 for hepatocytes, LSECs, and Kupffer cells (KCs), respectively. Data are depicted as mean ± standard deviation of the percentage ^{125}I counted per cell type of total radioactivity recovered.

clearance to the same extent as full-length VWF (Fig. S5). Brightfield microscopy showed that the majority of rFVIII was in non-hepatocyte cells, with less intense staining in hepatocytes, reminiscent of intracellular vesicles and bile canaliculi (Fig. 5A,B). Coformulation of FVIII with D′D3A1 did not appear to alter the relative distribution of rFVIII between cell types (although less overall FVIII staining was observed), indicating that VWF binding decreases FVIII clearance without altering the relative distribution of FVIII between liver cells (Fig. 5C).

To further distinguish between the different cell types within the sinusoids, histologic sections were costained for FVIII and CD68 (KC marker) or CD31 (endothelial marker) by the use of double immunofluorescence. The most intense FVIII staining was found in LSECs, with less FVIII staining of KCs being observed (Fig. 5E–J). No staining was observed when primary antibodies were replaced with unspecific IgG (data not shown). As seen with brightfield microscopy, FVIII staining in structures resembling bile canaliculi and intracellular vesicles within hepatocytes was also observed by immunofluorescence microscopy when the sensitivity was increased (data not shown). These immunohistochemical data correlate with the hepatocellular cell isolation data, supporting a role for LSECs and hepatocytes in the clearance of FVIII.

Discussion

The *in vivo* stability of glycoiodinated FVIII molecules was demonstrated in rats, and found to be superior to that achieved with commonly used methods, which rely on random oxidative radioiodination of tyrosines [18–20], possibly affecting bioactivity or binding, and rendering radioiodinated proteins susceptible to cleavage by deiodinases. This results in less accurate localization of the radiolabeled probe just a few hours after administration [21,22]. Glycoiodination is based on site-selective conjugation, and allows for comparable *in vitro* and *in vivo* FVIII characteristics. The majority of iodine (94%) was bound to FVIII during circulation *in vivo*, and > 1% was detected in the thyroid after 16 h.

^{125}I-rFVIII and ^{125}I-FVIII-Y1680F, the latter with strongly reduced VWF binding, as confirmed in VWF-binding and cell-binding assays, were used to study the influence of high-affinity VWF binding on FVIII distribution in rats after intravenous injection. Approximately 50% of the administered radioactivity was recovered 1 h after injection for both ^{125}I-rFVIII and ^{125}I-FVIII-Y1680F. These data are similar to the recovery data for other ^{125}I-labeled proteins, where unrecovered radioactivity may be non-specifically bound to carcass tissue [42], or eliminated via the urine or feces [43]. The majority of ^{125}I-rFVIII was recovered in the liver, followed by the intestines. A peak of ^{125}I-rFVIII radioactivity in the small and large intestines (total 30% ± 4%) was observed at 8 h, and decreased thereafter. In comparison with ^{125}I-rFVIII levels in the liver, this peak appears to be delayed, suggesting that the radioactivity detected in the intestines may be attributable to secretion of FVIII by hepatocytes via the bile duct, which subsequently empties directly into the duodenum in rats, and not into the gall bladder as in mice [44]. This metabolic pathway has previously been suggested for proteins, including IgA and activated FVII [39,43]. Radioactivity in the intestines could also be attributable to metabolized or deradioiodinated ^{125}I-FVIII from sites including the liver, and transported in the circulation. Deradioiodination is expected to be minimal, owing to the glycoiodination labeling of FVIII. ^{125}I-FVIII-Y1680F was also detected in the liver and gastrointestinal tract (albeit to a lesser extent), suggesting a distribution comparable to that of rFVIII. The

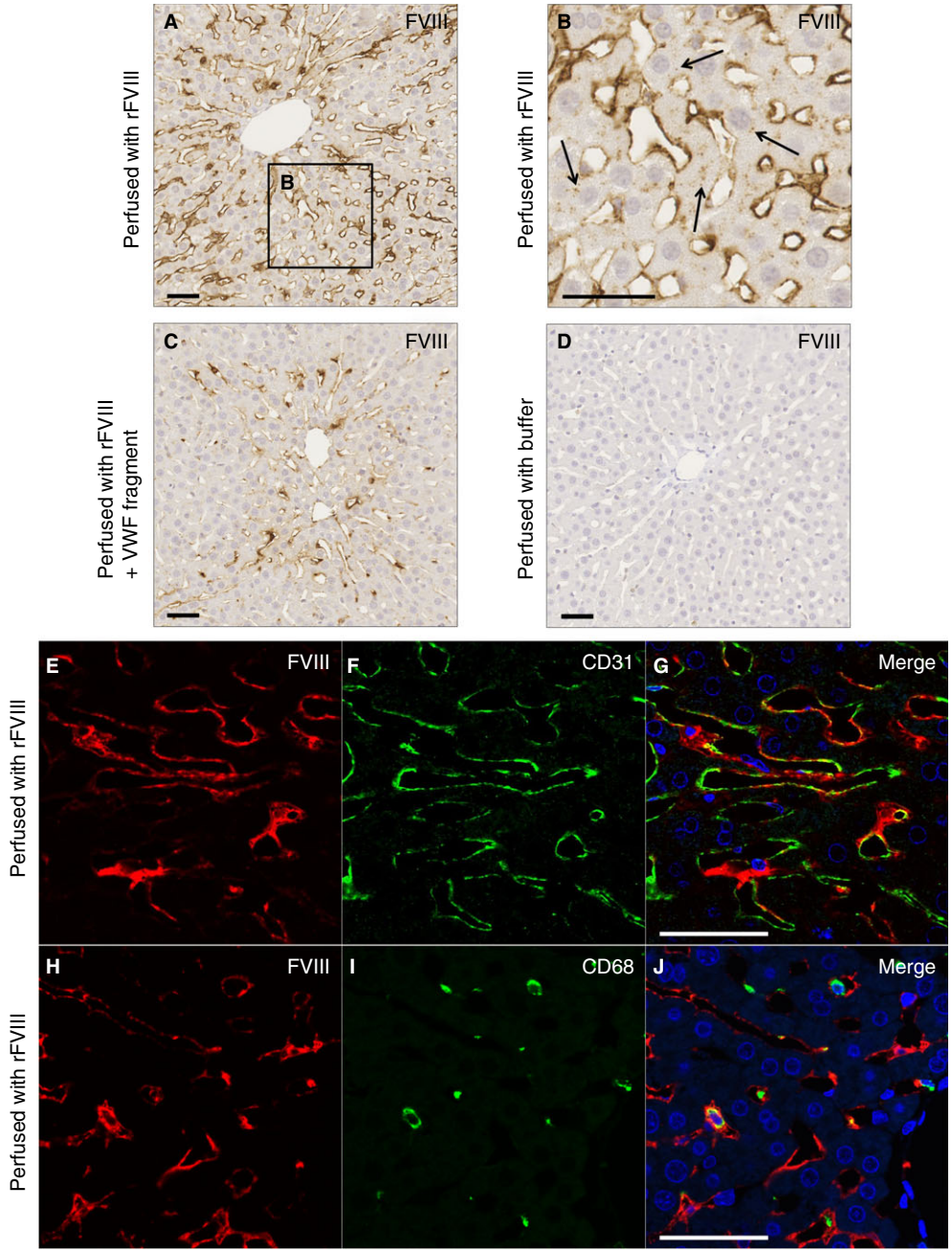

Fig. 5. Recombinant FVIII (rFVIII) detected in hepatocytes, liver sinusoidal endothelial cells (LSECs), and Kupffer cells (KCs). Histologic sections of rat liver perfused *ex vivo* with 20 nM human rFVIII were stained for FVIII with an antibody that does not detect endogenous rat FVIII. (A, B) Brightfield microscopy of rFVIII-perfused rat liver stained for rFVIII. The most intense rFVIII staining was found in the liver sinusoids containing LSECs and KCs. Less intense, punctate staining reminiscent of bile canaliculi and vesicles was also observed in hepatocytes (shown by arrows in [B]). (C) Rat liver perfused with rFVIII coformulated with a von Willebrand factor (VWF) fragment, D′D3A1, containing the FVIII-binding domains, D′D3, showed a similar FVIII staining pattern as when perfused with FVIII alone, albeit that less FVIII appears to be detected. (D) Rat liver perfused with vehicle buffer alone showed no staining of FVIII, confirming that the anti-FVIII antibody detects only human rFVIII and not endogenous rat FVIII. (E–G) Double immunofluorescence staining for rFVIII and the LSEC marker CD31, showing that the majority of rFVIII detected is found in LSECs. (H–J) Double immunofluorescence staining for rFVIII and the KC marker CD68, showing that a small fraction of KCs have also taken up rFVIII. Scale bars: 50 μm.

lower level of radioactivity in the intestines for ^{125}I-FVIII-Y1680F than for ^{125}I-rFVIII may be attributable to decreased secretion into the bile by hepatocytes. Although the kinetics of the distributions of rFVIII and FVIII-Y1680F cannot be directly compared, owing to the shorter $t_{1/2}$ of FVIII-Y1680F, these data suggest that VWF does not alter the anatomical distribution of FVIII in rats.

Previously, both the liver and spleen have been described as being important organs in the clearance of

FVIII [16,17]. In the present study, uptake of rFVIII by the spleen was also observed in both the presence and the absence of high-affinity VWF binding, with significant radioactivity per gram of tissue being observed. However, as the spleen is much smaller than the liver, the latter is believed to play a larger role in FVIII clearance and metabolism.

Both hepatocellular distribution studies reported here support a predominant role for hepatocytes and LSECs in the clearance of FVIII, independently of high-affinity binding to VWF. Hepatocellular cell isolation studies demonstrated that ~60% of rFVIII and FVIII-Y1680F were located in hepatocytes and ~35% in LSECs, following *in vivo* dosing of FVIII. These findings are consistent with the abundant expression of one of the receptors involved in FVIII clearance, LRP, on both hepatocytes [45] and LSECs [46]. LRP is involved in FVIII clearance either directly [47–49] or indirectly, via flow-dependent uptake of FVIII bound to VWF [50]. When the amount of radioactivity per million cells was quantified, LSECs were associated with significantly more FVIII at 7 h than were hepatocytes, and the same was true for FVIII-Y1680F at all time-points. This may indicate that LSECs have a greater capacity for clearance than hepatocytes, but does not diminish the significance of hepatocytes in the clearance and/or metabolism of FVIII, owing to their larger volume, larger size and greater abundance than LSECs.

The importance of both LSECs and hepatocytes in the clearance of FVIII, in the presence of VWF, has not been previously reported. Rather, KCs have been identified as being primarily responsible for the uptake of FVIII in the presence of VWF [17]. In the absence of VWF, e.g. in VWF knockout mice, FVIII is detected primarily in hepatocytes [17]. In the present study, a contribution by KCs was observed, but it appears to be minimal in comparison with hepatocytes and LSECs. The differences between previously published data and those reported here may be attributable to variations in animal models and methodologies, including different dosing levels of FVIII. Instead of using VWF knockout mouse models to represent the absence of VWF, we used the FVIII-Y1680F mutant, with reduced binding to VWF, in a rodent model with endogenous VWF. A similar distribution would be expected in rats with hemophilia A, as VWF in plasma from normal rats and from those with hemophilia A binds rFVIII in a comparable manner. Additionally, doses in the present studies are within the dose linearity range observed in mice [51], indicating that the rFVIII doses used are not saturating clearance mechanisms.

In conclusion, the present study confirms a primary role for the liver in FVIII clearance, and demonstrates that some of the dosed FVIII was also in the gastrointestinal tract, being potentially secreted via the bile. Both hepatocytes and LSECs appear to have major roles in FVIII clearance, with KCs making a minor contribution. Although VWF delays the clearance of FVIII, it does not affect the distribution or overall clearance pathway of FVIII. Further investigations are needed to delineate the relative involvement of different receptors in the cellular uptake of FVIII, in the absence and presence of VWF binding.

Addendum

C. I. Øie performed all anatomical distribution studies and the majority of the hepatocellular distribution studies and contributed to the writing and editing of the manuscript. K. Roepstorff performed the immunohistochemical study, and contributed to the writing and editing of the manuscript. C. Behrens and J. B. Kristensen created the novel glycoiodonation method and delivered the labeled proteins. D. M. Karpf performed PK studies and analysed their results. G. Bolt made FVIII and the FVIII-Y1680F variant. C. N. Gudme performed the *in vitro* cell-binding assays and antigen assays of the labeled proteins. M. Kjalke performed the VWF-binding assay, provided valuable scientific input to the overall study, and contributed to the writing and editing of the manuscript. B. Smedsrød provided valuable scientific input to the liver cell biology, supervised the anatomical and the hepatocellular distribution studies, and contributed to the writing and editing of the manuscript. R. S. Appa conceived the majority of the study design, was responsible for the *in vivo* studies, initiated the development of the glycoiodination method of labeling, and contributed to the writing and editing of the manuscript. All authors gave final approval of the version to be published.

Acknowledgements

A. Heerwagen, A. Larsen, K. Meeske, S. Kryger, B. Lassen, S. Bak, H. Rosenquist and L. Odborg of Novo Nordisk are thanked for expert technical assistance. K. Lester and J. Davies from AXON Communications are thanked for medical writing services.

Disclosure of Conflict of Interests

K. Roepstorff, C. Behrens, J. B. Kristensen, D. M. Karpf, G. Bolt, M. Kjalke, C. N. Gudme and R. S. Appa are employees of Novo Nordisk, and C. I. Øie has received honoraria from Novo Nordisk. B. Smedsrød and C. I. Øie report receiving salaries from the University of Tromsø, for tasks outside the submitted work. This research was funded by Novo Nordisk.

Supporting Information

Additional Supporting Information may be found in the online version of this article:

Fig. S1. Endogenous rat FVIII did not limit the capacity of the rat's VWF to bind human rFVIII.

Fig. S2. Glycoiodination did not alter FVIII plasma profiles.
Fig. S3. Glycoiodinated rFVIII was more stable than lactoperoxidase-labeled rFVIII.
Fig. S4. *Ex vivo*-perfused rat liver model.
Fig. S5. The VWF D′D3A1 fragment had a similar effect on rFVIII clearance as full-length VWF.

References

1 Kaufman RJ. Biological regulation of factor VIII activity. *Annu Rev Med* 1992; **43**: 325–39.
2 Berntorp E, Shapiro AD. Modern haemophilia care. *Lancet* 2012; **379**: 1447–56.
3 Shahani T, Covens K, Lavend'homme R, Jazouli N, Sokal E, Peerlinck K, Jacquemin M. Human liver sinusoidal endothelial cells but not hepatocytes contain factor VIII. *J Thromb Haemost* 2014; **12**: 36–42.
4 Hellman L, Smedsrod B, Sandberg H, Pettersson U. Secretion of coagulant factor VIII activity and antigen by *in vitro* cultivated rat liver sinusoidal endothelial cells. *Br J Haematol* 1989; **73**: 348–55.
5 Fahs SA, Hille MT, Shi Q, Weiler H, Montgomery RR. A conditional knockout mouse model reveals endothelial cells as the principal and possibly exclusive source of plasma factor VIII. *Blood* 2014; **123**: 3706–13.
6 Lenting PJ, van Schooten CJ, Denis CV. Clearance mechanisms of von Willebrand factor and factor VIII. *J Thromb Haemost* 2007; **5**: 1353–60.
7 Terraube V, O'Donnell JS, Jenkins PV. Factor VIII and von Willebrand factor interaction: biological, clinical and therapeutic importance. *Haemophilia* 2010; **16**: 3–13.
8 Tang L, Leong L, Sim D, Ho E, Gu JM, Schneider D, Feldman RI, Monteclaro F, Jiang H, Murphy JE. von Willebrand factor contributes to longer half-life of PEGylated factor VIII *in vivo*. *Haemophilia* 2013; **19**: 539–45.
9 Yee A, Gildersleeve RD, Gu S, Kretz CA, McGee BM, Carr KM, Pipe SW, Ginsburg D. A von Willebrand factor fragment containing the D′D3 domains is sufficient to stabilize coagulation factor VIII in mice. *Blood* 2014; **124**: 445–52.
10 Tuddenham EG, Lane RS, Rotblat F, Johnson AJ, Snape TJ, Middleton S, Kernoff PB. Response to infusions of polyelectrolyte fractionated human factor VIII concentrate in human haemophilia A and von Willebrand's disease. *Br J Haematol* 1982; **52**: 259–67.
11 Fray PJ. Factor VIII structure and function. *Int J Hematol* 2006; **83**: 103–8.
12 Fischer K, Pendu R, van Schooten CJ, van Dijk K, Denis CV, van den Berg HM, Lenting PJ. Models for prediction of factor VIII half-life in severe haemophiliacs: distinct approaches for blood group O and non-O patients. *PLoS ONE* 2009; **4**: e6745.
13 Leyte A, van Schijndel HB, Niehrs C, Huttner WB, Verbeet MP, Mertens K, van Mourik JA. Sulfation of Tyr1680 of human blood coagulation factor VIII is essential for the interaction of factor VIII with von Willebrand factor. *J Biol Chem* 1991; **266**: 740–6.
14 Michnick DA, Pittman DD, Wise RJ, Kaufman RJ. Identification of individual tyrosine sulfation sites within factor VIII required for optimal activity and efficient thrombin cleavage. *J Biol Chem* 1994; **269**: 20095–102.
15 Schwaab R, Oldenburg J, Schwaab U, Johnson DJ, Schmidt W, Olek K, Brackman HH, Tuddenham EG. Characterization of mutations within the factor VIII gene of 73 unrelated mild and moderate haemophiliacs. *Br J Haematol* 1995; **91**: 458–64.
16 van Schooten CJ, Shahbazi S, Groot E, Oortwijn BD, van den Berg HM, Denis CV, Lenting PJ. Macrophages contribute to the cellular uptake of von Willebrand factor and factor VIII *in vivo*. *Blood* 2008; **112**: 1704–12.
17 van der Flier A, Liu Z, Tan S, Chen K, Drager D, Liu T, Patarroyo-White S, Jiang H, Light DR. FcRn rescues recombinant factor VIII Fc fusion protein from a VWF independent FVIII clearance pathway in mouse hepatocytes. *PLoS ONE* 2015; **10**: e0124930.
18 Marchalonis JJ. An enzymic method for the trace iodination of immunoglobulins and other proteins. *Biochem J* 1969; **113**: 299–305.
19 Greenwood FC, Hunter WM. The preparation of 131I-labelled human growth hormone of high specific radioactivity. *Biochem J* 1963; **89**: 114–23.
20 Fraker PJ, Speck JC Jr. Protein and cell membrane iodinations with a sparingly soluble chloroamide, 1,3,4,6-tetrachloro-3α, 6α-diphenylglycoluril. *Biochem Biophys Res Commun* 1978; **80**: 849–57.
21 Awasthi V, Meinken G, Springer K, Srivastava SC, Freimuth P. Biodistribution of radioiodinated adenovirus fiber protein knob domain after intravenous injection in mice. *J Virol* 2004; **78**: 6431–8.
22 Hellevik T, Bondevik A, Smedsrod B. Intracellular fate of endocytosed collagen in rat liver endothelial cells. *Exp Cell Res* 1996; **223**: 39–49.
23 Thim L, Vandahl B, Karlsson J, Klausen NK, Pedersen J, Krogh TN, Kjalke M, Petersen JM, Johnsen LB, Bolt G, Nørby PL, Steenstrup TD. Purification and characterization of a new recombinant factor VIII (N8). *Haemophilia* 2010; **16**: 349–59.
24 Wilbur DS, Hadley SW, Hylarides MD, Abrams PG, Beaumier PA, Morgan AC, Reno JM, Fritzberg AR. Development of a stable radioiodinating reagent to label monoclonal antibodies for radiotherapy of cancer. *J Nucl Med* 1989; **30**: 216–26.
25 Vaidyanathan G, Zalutsky MR. Preparation of N-succinimidyl 3-[*I]iodobenzoate: an agent for the indirect radioiodination of proteins. *Nat Protoc* 2006; **1**: 707–13.
26 Christiansen ML, Balling KW, Persson E, Hilden I, Bagger-Sorensen A, Sorensen BB, Viuff D, Segel S, Klausen NK, Ezban M, Lethagen S, Steenstrup TD, Kjalke M. Functional characteristics of N8, a new recombinant FVIII. *Haemophilia* 2010; **16**: 878–87.
27 Stennicke HR, Kjalke M, Karpf DM, Balling KW, Johansen PB, Elm T, Ovlisen K, Moller F, Holmberg HL, Gudme CN, Persson E, Hilden I, Pelzer H, Rahbek-Nielsen H, Jespersgaard C, Bogsnes A, Pedersen AA, Kristensen AK, Peschke B, Kappers W, *et al*. A novel B-domain O-glycoPEGylated FVIII (N8-GP) demonstrates full efficacy and prolonged effect in hemophilic mice models. *Blood* 2013; **121**: 2108–16.
28 Jacobs DI, van Rijssen MS, van der Heijden R, Verpoorte R. Sequential solubilization of proteins precipitated with trichloroacetic acid in acetone from cultured Catharanthus roseus cells yields 52% more spots after two-dimensional electrophoresis. *Proteomics* 2001; **1**: 1345–50.
29 Peterson GL. Determination of total protein. *Methods Enzymol* 1983; **91**: 95–119.
30 Sivaraman T, Kumar TK, Jayaraman G, Yu C. The mechanism of 2,2,2-trichloroacetic acid-induced protein precipitation. *J Protein Chem* 1997; **16**: 291–7.
31 Elvevold K, Simon-Santamaria J, Hasvold H, McCourt P, Smedsrod B, Sorensen KK. Liver sinusoidal endothelial cells depend on mannose receptor-mediated recruitment of lysosomal enzymes for normal degradation capacity. *Hepatology* 2008; **48**: 2007–15.
32 Waynforth HB, Flecknell PA. *Experimental and Surgical Technique in the Rat*. San Diego, CA: Academic Press, 1992:342.
33 Smedsrød B, Pertoft H. Preparation of pure hepatocytes and reticuloendothelial cells in high yield from a single rat liver by means of Percoll centrifugation and selective adherence. *J Leukoc Biol* 1985; **38**: 213–30.

34 Melkko J, Hellevik T, Risteli L, Risteli J, Smedsrød B. Clearance of NH2-terminal propeptides of types I and III procollagen is a physiological function of the scavenger receptor in liver endothelial cells. *J Exp Med* 1994; **179**: 405–12.

35 Smedsrød B, Melkko J, Risteli L, Risteli J. Circulating C-terminal propeptide of type I procollagen is cleared mainly via the mannose receptor in liver endothelial cells. *Biochem J* 1990; **271**: 345–50.

36 van Berkel TJ, van Velzen A, Kruijt JK, Suzuki H, Kodama T. Uptake and catabolism of modified LDL in scavenger-receptor class A type I/II knock-out mice. *Biochem J* 1998; **331**: 29–35.

37 Hansen B, Longati P, Elvevold K, Nedredal GI, Schledzewski K, Olsen R, Falkowski M, Kzhyshkowska J, Carlsson F, Johansson S, Smedsrød B, Goerdt S, Johansson S, McCourt P. Stabilin-1 and stabilin-2 are both directed into the early endocytic pathway in hepatic sinusoidal endothelium via interactions with clathrin/AP-2, independent of ligand binding. *Exp Cell Res* 2005; **303**: 160–73.

38 Pertoft H, Smedsrød B. Separation and characterization of liver cells. In: Pretlow TGI, Pretlow TP, eds. *Cell Separation: Methods and Selected Applications*. New York: Academic Press, 1987: 1–24.

39 Appa R, Theill C, Hansen L, Moss J, Behrens C, Nicolaisen EM, Klausen NK, Christensen MS. Investigating clearance mechanisms for recombinant activated factor VII in a perfused liver model. *Thromb Haemost* 2010; **104**: 243–51.

40 Bloem E, van den Biggelaar M, Wroblewska A, Voorberg J, Faber JH, Kjalke M, Stennicke HR, Mertens K, Meijer AB. Factor VIII C1 domain spikes 2092–2093 and 2158–2159 comprise regions that modulate cofactor function and cellular uptake. *J Biol Chem* 2013; **288**: 29670–9.

41 Takahashi Y, Kalafatis M, Girma JP, Sewerin K, Andersson LO, Meyer D. Localization of a factor VIII binding domain on a 34 kilodalton fragment of the N-terminal portion of von Willebrand factor. *Blood* 1987; **70**: 1679–82.

42 Elvevold K, Simon-Santamaria J, Hasvold H, McCourt P, Smedsrod B, Sorensen KK. Liver sinusoidal endothelial cells depend on mannose receptor-mediated recruitment of lysosomal enzymes for normal degradation capacity. *Hepatology* 2008; **48**: 2007–15.

43 Orlans E, Peppard J, Reynolds J, Hall J. Rapid active transport of immunoglobulin A from blood to bile. *J Exp Med* 1978; **147**: 588–92.

44 McMaster PD. Do species lacking a gall bladder possess its functional equivalent? *J Exp Med* 1922; **35**: 127–40.

45 Kim C, Vaziri ND. Down-regulation of hepatic LDL receptor-related protein (LRP) in chronic renal failure. *Kidney Int* 2005; **67**: 1028–32.

46 Øie CI, Appa RS, Hilden I, Petersen HH, Gruhler A, Smedsrod B, Hansen JB. Rat liver sinusoidal endothelial cells (LSECs) express functional low density lipoprotein receptor-related protein-1 (LRP-1). *J Hepatol* 2011; **55**: 1346–52.

47 Lenting PJ, Neels JG, van den Berg BM, Clijsters PP, Meijerman DW, Pannekoek H, van Mourik JA, Mertens K, van Zonneveld AJ. The light chain of factor VIII comprises a binding site for low density lipoprotein receptor-related protein. *J Biol Chem* 1999; **274**: 23734–9.

48 Saenko EL, Yakhyaev AV, Mikhailenko I, Strickland DK, Sarafanov AG. Role of the low density lipoprotein-related protein receptor in mediation of factor VIII catabolism. *J Biol Chem* 1999; **274**: 37685–92.

49 Schwarz HP, Lenting PJ, Binder B, Mihaly J, Denis C, Dorner F, Turecek PL. Involvement of low-density lipoprotein receptor-related protein (LRP) in the clearance of factor VIII in von Willebrand factor-deficient mice. *Blood* 2000; **95**: 1703–8.

50 Rastegarlari G, Pegon JN, Casari C, Odouard S, Navarrete AM, Saint-Lu N, van Vlijmen BJ, Legendre P, Christophe OD, Denis CV, Lenting PJ. Macrophage LRP1 contributes to the clearance of von Willebrand factor. *Blood* 2012; **119**: 2126–34.

51 Elm T, Karpf DM, Ovlisen K, Pelzer H, Ezban M, Kjalke M, Tranholm M. Pharmacokinetics and pharmacodynamics of a new recombinant FVIII (N8) in haemophilia A mice. *Haemophilia* 2012; **18**: 139–45.